



INVESTIGATION OF LINEAR AND NONLINEAR BEHAVIOUR OF REINFORCED CONCRETE COLUMN EXPOSED TO CORROSION EFFECT FOR DIFFERENT DAMAGE LIMIT LEVELS

Halit Erdem ÇOLAKOĞLU^{1*}, Muhammed ÖZTEMEL¹


¹Giresun University, Vocational High School of Keşap, Department of Building, 28000, Giresun, Türkiye


Abstract: The high performance of reinforced concrete structural elements under the effects of lateral loads such as earthquakes is of great importance in terms of minimizing the loss of life and property that may occur due to earthquakes. One of the parameters affecting the earthquake behavior of a reinforced concrete structure is the corrosion effect. The aim of this study is to investigate the behavior of reinforced concrete columns exposed to different corrosion levels for different durations within the damage limits. In this direction, it is aimed to perform linear and nonlinear analysis of reinforced concrete columns in 5 different corrosion scenarios. In the study, nonlinear analyzes of the column were made using ANSYS software, the data obtained were determined for different damage limit levels and compared with the section analysis. Because of the study, moment-curvature relations, lateral load-horizontal displacement relations, bending ductility and plastic rotation capacity of the reinforced concrete column were determined for each corrosion scenario.

Keywords: Corrosion, Propagation velocity, Impact time, Plastic rotation, Flexural ductility

*Corresponding author: Giresun University, Vocational High School of Keşap, Department of Building, 28000, Giresun, Türkiye

E mail: haliterdemcolakoglu@gmail.com (H. E. ÇOLAKOĞLU)

Halit Erdem ÇOLAKOĞLU  <https://orcid.org/0000-0002-4498-3569>

Muhammed ÖZTEMEL  <https://orcid.org/0000-0002-6530-0739>

Received: January 24, 2024

Accepted: March 20, 2024

Published: May 15, 2024

Cite as: Çolakoğlu HE, Öztemel M. 2024. Investigation of linear and nonlinear behaviour of reinforced concrete column exposed to corrosion effect for different damage limit levels. BSJ Eng Sci, 7(3): 409-422.

1. Introduction

Reinforcement corrosion occurring in a reinforced concrete structure causes cracking and spalling in the concrete by decreasing the diameter of the reinforcement, loss of adherence between concrete and reinforcement and decrease in the mechanical properties of reinforcing steel, thus decreasing the performance of the carrier system. In reinforced concrete columns and beams exposed to corrosion effect, since volume expansions occur due to excessive corrosion of the reinforcement, corrosion cracks in the longitudinal direction cause the strut layer to break off in time (Figure 1). Reinforced concrete structures subjected to these corrosion effects reach the state of collapse in a much shorter time than normal and in abnormal ways under the effect of earthquake loads.



Figure 1. Reinforced concrete elements subjected to corrosion effect.

When the literature examined, many experimental and numerical studies have carried out on the effects of corrosion on reinforcing steel and the inadequacies in earthquake performance due to the negative effects of corrosion on reinforced concrete structures. In these studies, it has been determined that the failure mode of beams subjected to corrosion under bending effect changes from ductile to brittle (Mangat and Elgarf, 1999; Mohammed et al., 2004). In addition, in these studies, it stated that corrosion of steel reinforcement causes deformation of the entire system, especially the bearing capacity of the structural elements (Yavuz et al., 2019). In studies evaluating the seismic performance of reinforced concrete columns at different corrosion levels and axial load rates, it was determined that the corrosion effect significantly reduces the strength and horizontal displacement capacity of the columns and changes the failure mode from flexural-shear failure to sudden axial failure (Vu and Li, 2018). Palsson and Mirza (2002) subjected reinforcing bar samples taken from reinforced concrete bridges subjected to corrosion to tensile tests and found that the reinforcements fractured brittle. Revathy et al. (2009) concluded that the axial load carrying capacity of column elements subjected to corrosion effect gradually decreases with increasing corrosion effect.

In case of weakening of the adherence bond established



between the reinforcement and concrete in the constituent elements of the reinforced concrete structure, the behavior of the reinforced concrete structure turns into a stressed arch behavior. In stressed arch behavior, since the reinforcement collapses before reaching the yield stress, the relationship between the corrosion level of the reinforcement and the adherence bond strength is extremely important. It was determined that at low corrosion levels, the adherence bond strength increased to a certain extent, but if the corrosion level increased, the adherence bond strength gradually decreased (Chung et al., 2008). This decrease in bond strength causes significant changes in the earthquake performance and target displacements of the structure (Yüksel and Sancaklı, 2018).

In columns where reinforcement losses due to corrosion increase up to 15.1%, the increase in corrosion level impairs the cyclic stability of the reinforced concrete column under cyclic load effects and reduces the ductility of the reinforced concrete column (Ying et al., 2012).

In some studies in the literature, the effect of corrosion on reinforced concrete structures has studied using finite element modeling technique. Dizaj and Kashani (2021) proposed a modeling technique that simulates the regional variability of corrosion and the effects of corrosion damage. Finite element analysis using the proposed modeling approach revealed that corrosion significantly affected the damage states, flexural capacity and energy absorption capacity of reinforced concrete members. In another study by Imperatore et al. (2017), where an experimental study to evaluate the residual flexural capacity of beams was simulated using the finite element method, the relationship between the level of corrosion and the reduction in the flexural strength of the

beam was determined (Bossio et al., 2019). In another study evaluating the seismic behavior of corroded reinforced concrete bridges, the decrease in the bond strength between concrete and reinforcement was modeled using finite element modeling technique. Softening of concrete and reduction in mechanical properties of reinforcement also taken into account in the modeling. Because of the study, it recommended to increase the design PGA from 4.70% to 6.15% for the seismic performance of the bridge considering the reductions due to corrosion effect. (Ou et al., 2013).

In this study, the linear and nonlinear behavior of reinforced concrete column elements under 5 different corrosion scenarios were investigated. In the corrosion scenarios, the adherence losses between reinforcement and concrete and all the consequences of corrosion on concrete and reinforcement elements modelled together depending on the corrosion propagation rate and corrosion duration parameters. In the study, the change in column structural behavior due to corrosion evaluated in terms of damage limits at different corrosion levels using both finite element method and cross-sectional analysis.

2. Materials and Methods

A reinforced concrete column with a rectangular cross-section of 300 x 400 x 2350 mm dimensions determined in accordance with TBDY (2018) used in the study. The concrete strength class of the column element taken as C25/30. The size information of the reinforced concrete column, the layout of the longitudinal and transverse reinforcements used and the variation of the transverse reinforcement spacing are as shown in Figure 2.

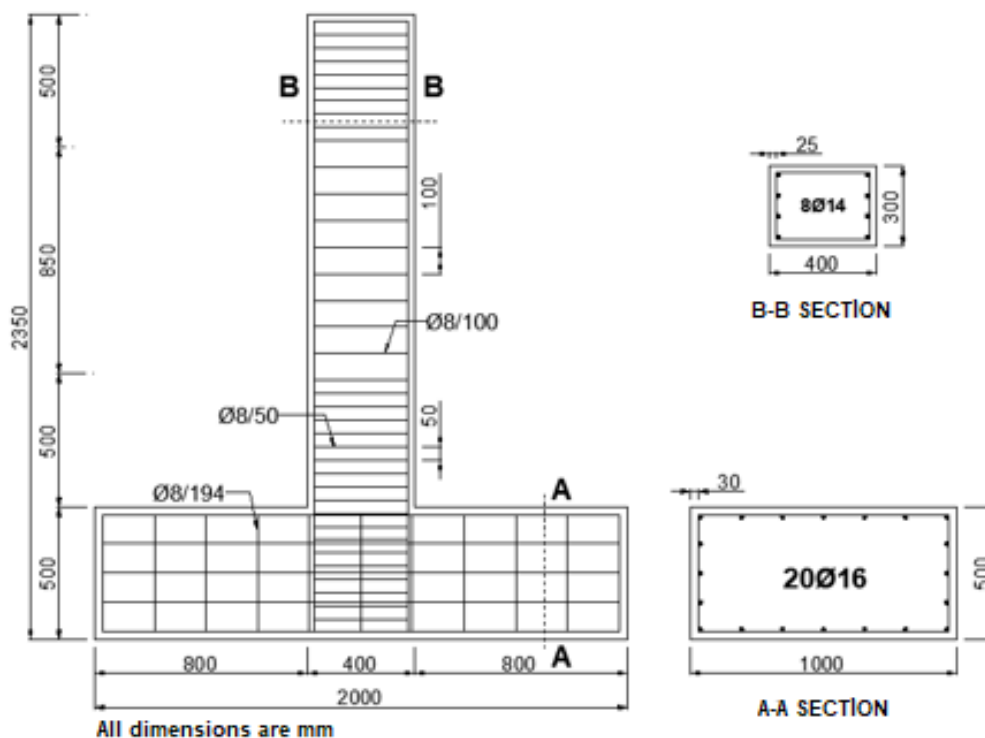


Figure 2. Reinforced concrete column cross-section and reinforcement arrangement.

TBDY, (2018) a 500 mm long formed at the upper and lower ends of the column, and no stirrup with a diameter smaller than Ø8 used as transverse reinforcement in these zones. According to TBDY (2018) the spacing of the transverse reinforcements to be used in the column is arranged so that they are not smaller than 50 mm and not larger than 100 mm. Reinforcement smaller than Ø14 was not used in the reinforced concrete column element, and the longitudinal reinforcement area specified in TBDY (2018) was acted in accordance with the condition that the longitudinal reinforcement area shall not be less than 1% and not greater than 4% of the gross cross section.

According to TBDY (2018) the longitudinal reinforcement ratio in column elements should not be less than 0.01 and not greater than 0.04. In this context, 8Ø14 longitudinal reinforcement used in the reinforced concrete column used in the study and the longitudinal reinforcement ratio calculated as 0.0103. Since the normal force determines the type of fracture in the reinforced concrete column element, the normal force should be limited to prevent brittle fracture (Topçu, 2022). According to TBDY (2018) the maximum axial load that the column element can carry calculated as stated in Equation 1.

$$N_d \leq 0,4f_{ck}A_c \quad (1)$$

According to Equation 1, the maximum axial load value that the reinforced concrete column used in the study can carry calculated as 1200 kN.

In this study, it investigated how the earthquake performance of the reinforced concrete column element, whose dimensional and cross-sectional properties given above, will change if it exposed to corrosion effect. In this context, the reinforced concrete column element was analyzed under 5 different corrosion scenarios. The effect of corrosion on the reinforced concrete column depends on the rate of corrosion spread and the duration of the effect, but it causes the steel reinforcement to expand in volume, soften and reduce its weight. The decrease in the weight and change in the diameter of the steel reinforcement calculated using Equation 2 and Equation 3 as follows (Berto et al., 2008):

$$\% \Delta_w = \frac{\phi_0^2 - \phi(t)^2}{\phi_0^2} \times 100 \quad (2)$$

$$\phi(t) = \phi_0 - 2P_x = \phi_0 - 2i_{corr}k(t - t_{in}) \quad (3)$$

2.1. Evaluation of the Rate of Propagation and Duration of Corrosion

In the literature, a number of formulations based mainly

on empirical expressions have been proposed for the evaluation of corrosion propagation rate (i_{corr}) and weight decrease in reinforcing steel, ranging from a deterministic approach to a probabilistic context (Berto et al., 2009). In particular, the evaluation of corrosion propagation rate (i_{corr}) obtained from laboratory tests and corrosion effects in real structures is shown in Table 1 (Dhir et al., 1994; Brite/Euram, 1995; Middleton and Hogg, 1998).

In this study, $i_{corr}=0.15$ for reinforced concrete columns with low corrosion level and $i_{corr}=0.8$ for reinforced concrete columns with medium corrosion level and $i_{corr}=4$ for reinforced concrete columns with high corrosion level and the current corrosion scenarios are shown in Table 2. In the study, 15 years since the reinforced concrete column was manufactured (t_{in}) was considered as the initial stage of corrosion.

In addition to the weight decrease in the reinforcing bar of a reinforced concrete column subjected to corrosion, some changes occur in the yield and tensile strengths, yield and tensile deformations and elastic modulus of the reinforcement in a corroded reinforcement. These changes calculated using Equation 4, Equation 5, Equation 6 and Equation 7 (Lee and Cho, 2009):

$$\sigma_y = \left(1 - 1,24 \cdot \frac{\Delta_w}{100}\right) \cdot \sigma_{y(initial)} \quad (4)$$

$$\sigma_u = \left(1 - 1,07 \cdot \frac{\Delta_w}{100}\right) \cdot \sigma_{u(initial)} \quad (5)$$

$$E_s = \left(1 - 0,75 \cdot \frac{\Delta_w}{100}\right) \cdot E_{s(initial)} \quad (6)$$

$$\varepsilon_u = \left(1 - 1,95 \cdot \frac{\Delta_w}{100}\right) \cdot \varepsilon_{u(initial)} \quad (7)$$

The effects of corrosion on the bond strength reduction of the steel reinforcement due to corrosion must also take into account. To account for the effects of corrosion on bond strength reduction in the analysis, the concept of equivalent unlimited length was used (Ou et al., 2010). According to this concept, the reduction in bond strength reflected in the models by multiplying the bond reduction coefficient (Φ) defined by Equation 8 by the stress-strain curve of steel.

$$\Phi = \frac{L_{eu}(\text{corrosion free reinforcement})}{L_{eu}(\text{corroded reinforcement})} \quad (8)$$

Here L_{eu} is the equivalent unlimited length derived from Equation 9.

$$L_{eu} = \frac{S_E}{\varepsilon_{sm}} \quad (9)$$

Table 1. Classification of corrosion propagation rate i_{corr} ($\mu A/cm^2$)

Corrosion level	Dhir et al. (1994)	Brite/Euram (1995)	Middleton and Hogg (1998)
Corrosion free	-	$i_{corr} < 0,1$	-
Low	$i_{corr} = 0.1$	$i_{corr} = 0.1 - 0.5$	$i_{corr} = 0.1 - 0.2$
Middle	$i_{corr} = 1$	$i_{corr} = 0.5 - 1$	$i_{corr} = 0.2 - 1$
High	$r > 10$	$i_{corr} > 1.0$	$i_{corr} > 1.0$

Table 2. Corrosion scenarios

Scenario number	Initial diameter (mm)	i_{corr} ($\mu A/cm^2$)	Time t (yil)	t_{in} (yil)	Last diameter (mm)	Weight reduction (%)
1	8	0	0	0	8.00	0.00
	14	0	0	0	14.00	0.00
2	8	4	20	15	7.60	9.75
	14	4	20	15	13.60	5.63
3	8	0.8	50	15	7.44	13.51
	14	0.8	50	15	13.44	7.84
4	8	4	50	15	5.20	57.75
	14	4	50	15	11.20	36.00
5	8	4	35	15	6.40	36.00
	14	4	35	15	12.40	21.55

Where S_E is the slip of a reinforcement in the critical section of a column cross-section ε_{sm} is the maximum strain in the reinforcement and the slip in the reinforcement estimated using Equation 10 and Equation 11 (Sezen and Setzler, 2008):

$$S_E = \frac{\varepsilon_{sm} L_{d1}}{2} \quad (\varepsilon_{sm} \leq \varepsilon_y) \quad (10)$$

$$S_E = \frac{\varepsilon_y L_{d1}}{2} + \frac{(\varepsilon_{sm} - \varepsilon_y) L_{d2}}{2} \quad (\varepsilon_{sm} > \varepsilon_y) \quad (11)$$

Here L_{d1} and L_{d2} is calculated using Equation 12 and Equation 13.

$$L_{d1} = \frac{f_{sm} d_b}{4\tau_{max}} \leq \frac{f_y d_b}{4\tau_{max}} \quad (12)$$

$$L_{d2} = \frac{(f_{sm} - f_y) d_b}{4\tau_f} \quad (13)$$

Where f_{sm} , is the maximum stress in the reinforcement, d_b , is the longitudinal reinforcement diameter, τ_{max} , is the bond strength and τ_f , is the residual friction bond strength. For reinforcement without corrosion effect, τ_{max} and τ_f values can be taken as $\sqrt{f_c}$ and $0.15\tau_{max}$ respectively. When the reduction in reinforcement weight exceeds 1.5%, the corrosion effect calculated according to Equation 14 (Bhargava et al., 2008). When the corrosion level is less than 1.5 %, the bond strength assumed to be equal to the corrosion-free value. Here τ_{maxo} , is the bond strength is assumed to be equal to the corrosion free value.

$$\tau_{max} = 1.346e^{-0.198\Delta_w(\%)} \tau_{maxo} \quad (14)$$

The stress-unit strain curves of the reinforcements in the reinforced concrete column subjected to corrosion effect arranged for each corrosion scenario by considering the decrease in the adherence bond strength (Figure 3).

Cracking and softening effects occurring in the concrete due to corrosion effect should also take into consideration in the reinforced concrete column element exposed to corrosion. The softening effect of concrete due to corrosion expressed by concrete softening coefficient (ζ). Concrete softening coefficient calculated according to Equation 15 (Ou et al., 2013).

$$\zeta = \frac{0.9}{\sqrt{1 + 600\varepsilon_r}} \quad (15)$$

Where ε_r the yield is strain of reinforcement and calculated according to Equation 16. Where b_0 is the perimeter length of the reinforced concrete column cross-section and $\sum w_{cr}$ is the total crack width in the concrete due to corrosion of longitudinal and transverse reinforcement (Ou et al., 2013). Each crack width w_{cr} calculated using Equation 17 (Molina et al., 1993) (Figure 4).

$$\varepsilon_r = \frac{\sum w_{cr}}{b_0} \quad (16)$$

$$w_{cr} = \pi \cdot (V_{rs} - 1) \cdot 2x \quad (17)$$

Here $2x$ is the reduction in the diameter of the steel reinforcement due to corrosion. The volume expansion of steel reinforcement due to corrosion causes softening and weight decrease (Figure 4). V_{rs} is the diameter expansion coefficient of steel reinforcement due to corrosion. For this study, $V_{rs} = 2$ (Ou et al., 2013) (Figure 4).

Considering the effects of cracking and softening of the concrete due to the corrosion effect in the reinforced concrete column element subjected to corrosion, Equation 18 and Equation 19 are used for the increasing and decreasing regions of the stress- strain relationship of concrete, respectively (Hsu, 1993).

$$\sigma = \zeta f'_c \left[2 \left(\frac{\varepsilon}{\zeta \varepsilon_0} \right) - \left(\frac{\varepsilon}{\zeta \varepsilon_0} \right)^2 \right] \quad (18)$$

$$\sigma = \zeta f'_c \left[1 - \left(\frac{\frac{\varepsilon}{\zeta \varepsilon_0} - 1}{\frac{2}{\zeta} - 1} \right)^2 \right] \quad (19)$$

Here, ε_0 is the unit strain value corresponding to the maximum stress in the stress-strain curve of concrete and it accepted as approximately 0.002.

In the study, the stress-strain curve of the concrete material for each corrosion scenario in the reinforced concrete column subjected to corrosion effect was determined by considering the effects of cracking and softening in the concrete (Figure 5).

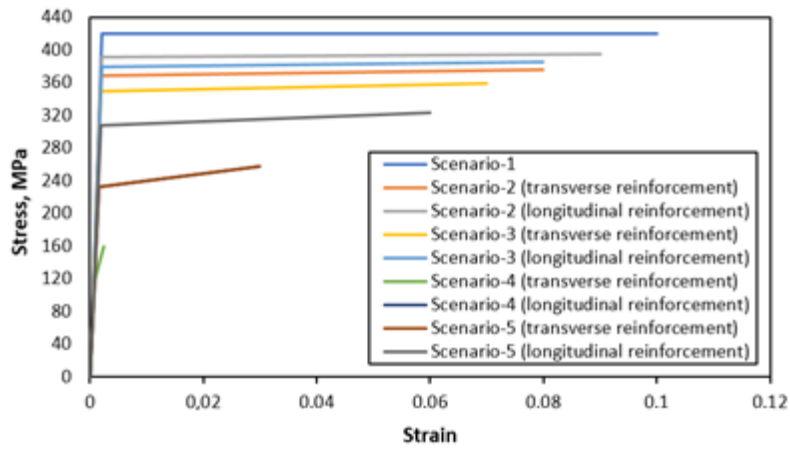


Figure 3. Stress - strain curves of steel according to corrosion scenarios.

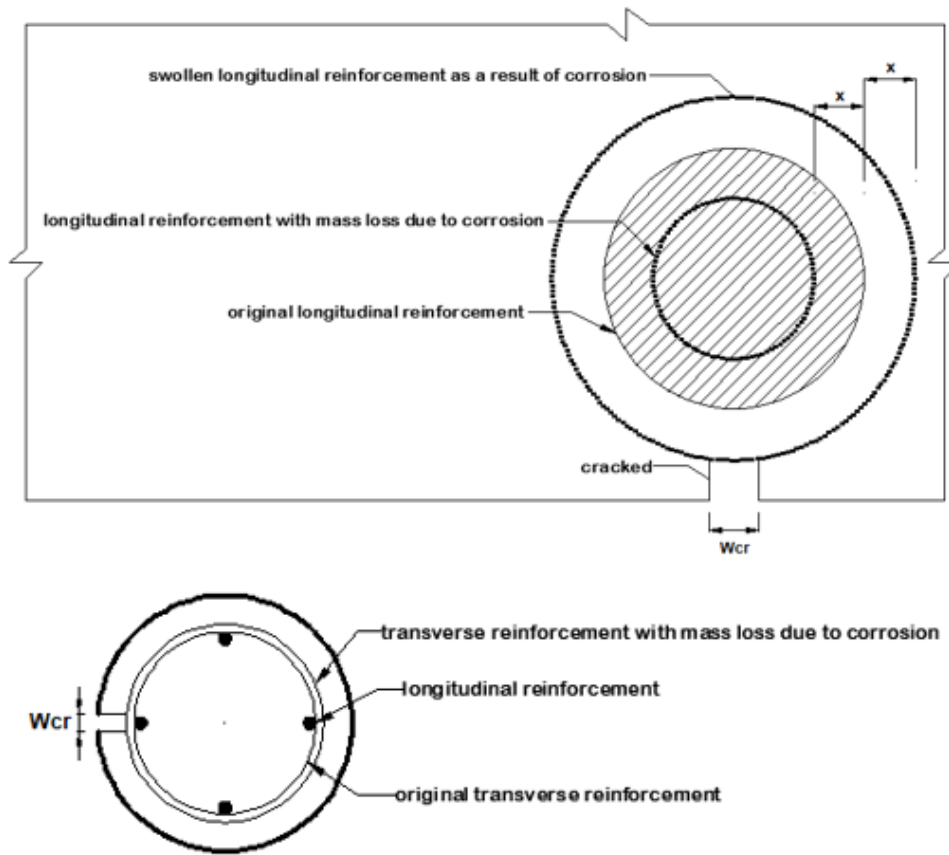


Figure 4. Corrosion cracks in longitudinal and transverse reinforcement.

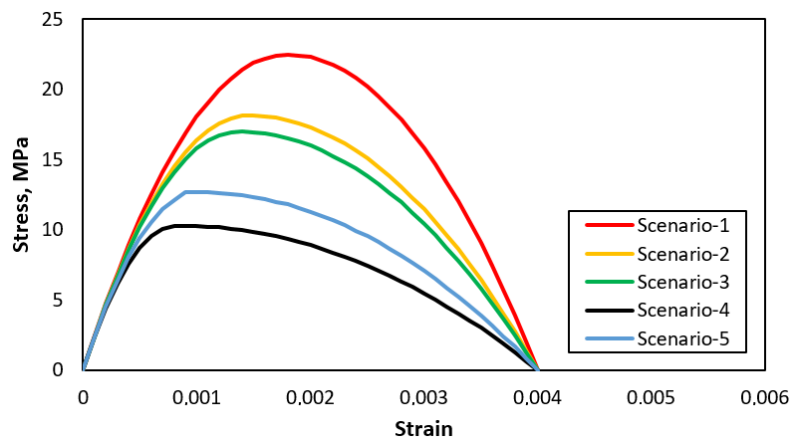


Figure 5. Stress - strain curves of concrete according to corrosion scenarios.

2.2. Creation of Finite Element Model of Reinforced Concrete Column

Finite element model of the reinforced concrete column element to be used in the study was created using ANSYS software. In the finite element model, Solid65, which is a solid element with 8 nodes, was used for concrete and Link180 elements were used for reinforcing steel. The finite element model of the reinforced concrete column shown in Figure 6.

In the finite element model, the foundation of the reinforced concrete column not modelled in order to shorten the analysis time and to create the minimum number of finite elements. Instead, each nodal point at

the lower end of the reinforced concrete column modelled in accordance with the anchored support assumption (Figure 7).

2.3. Determination of Stress-Strain Relationships for Concrete and Steel in Finite Element Model

The stress-strain curves of the concrete used in the finite element model of the reinforced concrete column shown in Figure 8 and the stress-strain curves of the reinforcing steel shown in Figure 3.

Concrete of strength class C25/30 used in the finite element model of the reinforced concrete column. The modulus of elasticity of concrete and steel material for different corrosion scenarios given in Table 3.

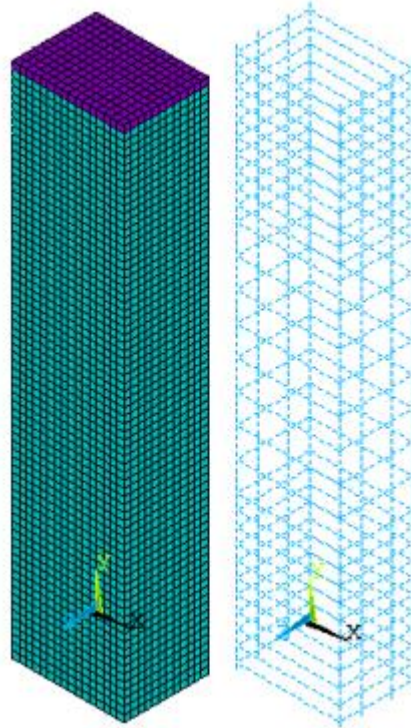


Figure 6. Reinforced concrete column concrete and reinforcement finite element model.

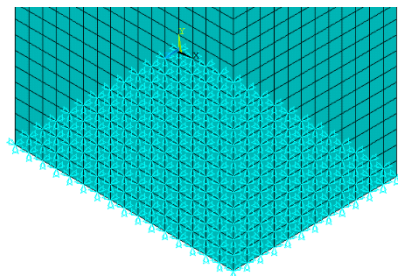


Figure 7. Reinforced concrete column anchored support model.

Table 3. Material properties according to corrosion scenarios (MPa)

Scenario number	Concrete (E_c)	Steel (E_s)	Concrete softening coefficient (α)
1	24306	200000	0.9
2	24139	188465	0.73
3	24080	183988	0.68
4	23483	129688	0.41
5	23767	156838	0.51

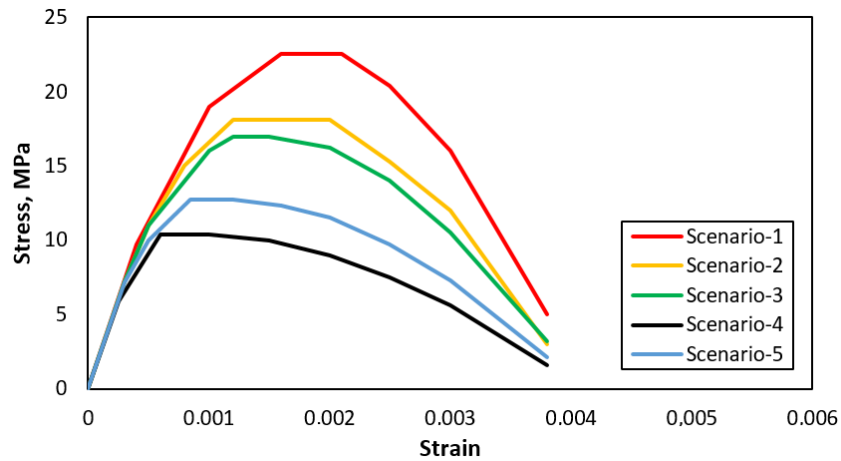


Figure 8. Concrete material models according to corrosion scenarios.

2.4. Application of Axial and Horizontal Load in Finite Element Model

In this study, the nonlinear behavior of a finite element modelled reinforced concrete column subjected to corrosion under axial load and lateral load investigated. For this purpose, 165 nodal points selected at the upper end of the column and the axial load $N_d = 1200 \text{ kN}$ equally distributed to each nodal point. In addition, horizontal displacement applied to a node at the upper end of the reinforced concrete column by utilizing the rigid beam feature of the MPC184 compliance element. The rigid beam feature of the MPC184 element utilized in order to distribute the applied lateral load equally and evenly to the reinforced concrete column and to prevent excessive deformation of the concrete particles forming the column nodes (Figure 9).

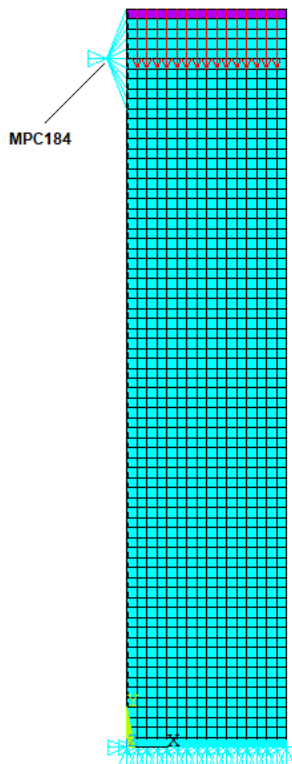


Figure 9. Application of axial load and lateral load.

2.5. Evaluation of the Reliability of the Finite Element Modelling Method Used

The reliability of the finite element modelling software used in the study and the demonstration that the parameters used in the modelling are determined in a way to give the closes results to the actual behavior of the reinforced concrete column are of great importance for the present study.

In the study conducted by Elçi and Göker (2018) the reinforced concrete column whose section geometry and reinforcement plan shown in Figure 10 was experimentally investigated under axial and lateral load. The existing reinforced concrete column was finite element modelled by Çolakoğlu (2020) and subjected to nonlinear analysis under the axial and horizontal load effects in the experimental study by Elçi and Göker (2018). The data obtained were processed and the shear force-horizontal displacement and bending moment-curvature relationships in Figure 11 were drawn.

When Figure 11 examined, it considered that the finite element modelling and nonlinear analysis performed with the ANSYS package are very reliable for reinforced concrete columns and it is important to adjust the modelling parameters to give results close to reality.

3. Results

In this study, nonlinear analysis of a reinforced concrete column whose finite element model produced using ANSYS software performed. In addition, cross-sectional analysis of the reinforced concrete column under corrosion effect performed and the deformation state compared with the nonlinear analysis. Lateral load – horizontal displacement relationship, bending moment-curvature relationship, flexural ductility and plastic rotation capacity evaluated using the obtained data.

3.1. Lateral Load - Horizontal Displacement Relationship

The horizontal load-lateral displacement graph obtained because of the nonlinear analysis of the reinforced concrete column subjected to corrosion effect under axial load and horizontal load shown in Figure 12 for each corrosion scenario.

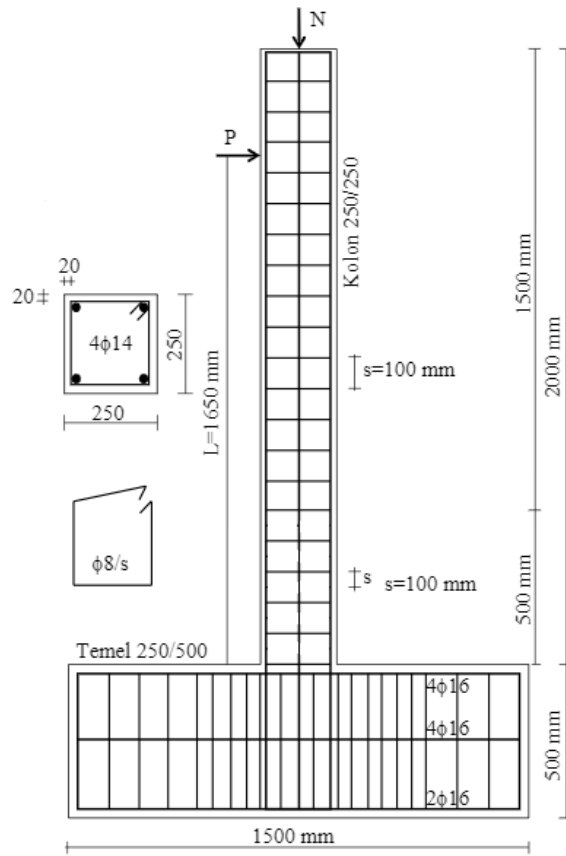


Figure 10. Reinforced concrete column cross-section and reinforcement plan.

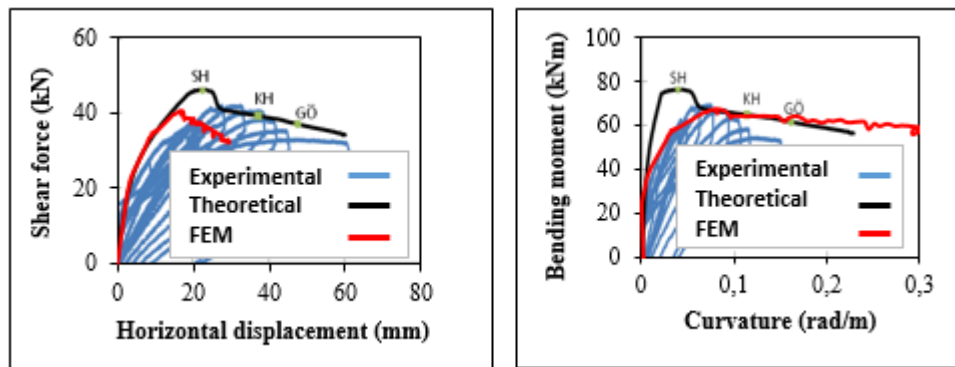


Figure 11. Shear force - horizontal displacement relationship and bending moment - curvature relationship.

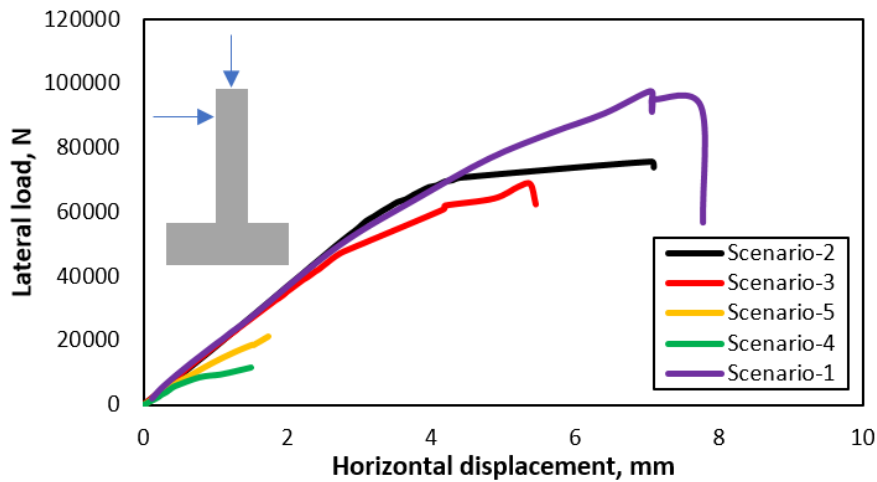


Figure 12. Lateral load - horizontal displacement relationship (ANSYS).

When Figure 12 analyzed, it seen that the lateral load capacity of the reinforced concrete column element exposed to corrosion effect decreases.

3.2. Bending Moment - Curvature Relationship

In order to determine the behavior of a section under the effect of bending and axial force or only bending, the moment-curvature relationship of a modelled element can be obtained based on the actual material behavior (Ersoy and Özcebe, 2018).

In order to calculate the values of M_i and K_i , which constitute the moment-curvature relationship, by iteration method, equations of equilibrium and compatibility are utilised. If a beam section is utilised, assumptions are made for the value of c (neutral axis depth), and the value of c is changed until the balance of forces is achieved. A value is chosen for the unit shortening of concrete at the outermost lift, ϵ_{ci} . Steel unit deformations, ϵ_{si} , are found for known ϵ_{ci} and c . Stresses in the reinforcement and reinforcement forces are determined from the ϵ_{si} values. The concrete compression component F_c is calculated. After equilibrium reached, the moment of internal forces around the centre of gravity is calculated and M_i found. The curvature is determined as given in Equation 20 (Ersoy and Özcebe, 2018).

$$K_i = \frac{\epsilon_{ci}}{c} \quad (20)$$

In the finite element model of the reinforced concrete column, the curvature calculated for each horizontal row of solid elements at the lower end of the column calculated as in Equation 21 by using the unit strains at the beginning and end nodes of each fibre as shown in Figure 13.

$$\phi = (|\epsilon_1| + |\epsilon_2|)/L \quad (21)$$

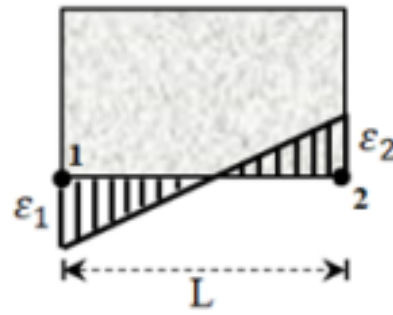


Figure 13. Definition of curvature in finite element modelling.

Figure 14 shows the bending moment-curvature relationship obtained from the nonlinear analysis of the reinforced concrete column subjected to corrosion effect, and Figure 15 shows the bending moment-curvature relationship obtained from the section calculation for each corrosion scenario.

When the lateral load - horizontal displacement relationship and bending moment - curvature relationship obtained from the nonlinear analysis of the reinforced concrete column subjected to corrosion effect were examined, it was determined that the lateral load capacity and moment carrying capacity decreased depending on the duration and rate of propagation of corrosion. This decrease found to be more intense especially in Scenario-4, where the rate of propagation and duration of corrosion was the highest.

When the cross-sectional analysis performed due to the corrosion effects to which the reinforced concrete column element was exposed were examined, it was determined that the moment carrying capacity and cross-sectional ductility decreased depending on the corrosion levels, similar to the results obtained in the nonlinear analysis.

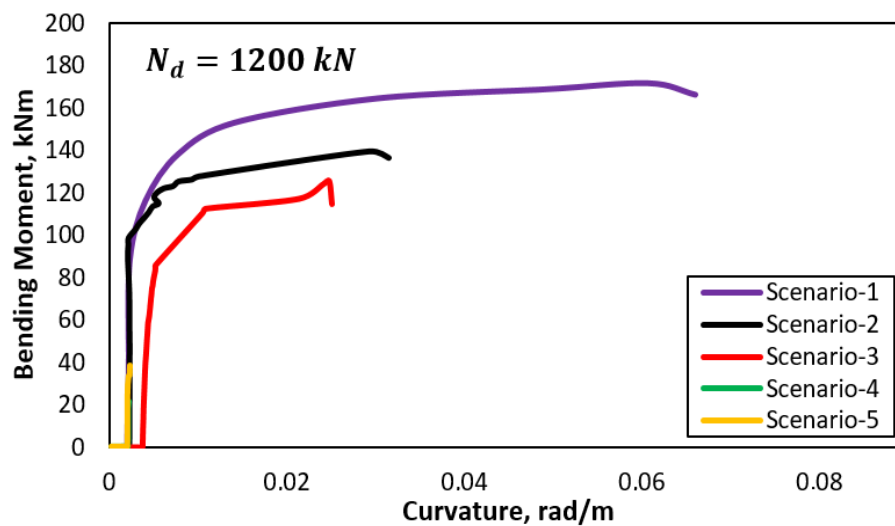


Figure 14. Bending moment - curvature relationship for nonlinear analyses (FEM)

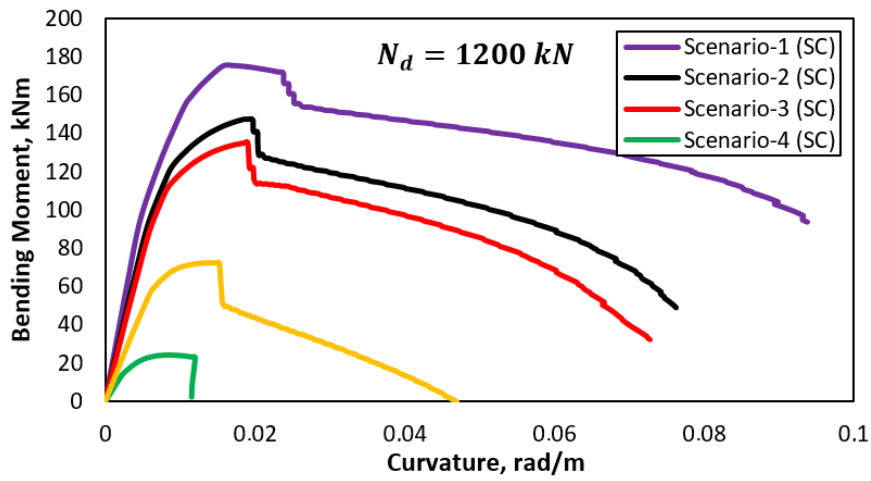


Figure 15. Bending moment – curvature relationship for section calculation (SC).

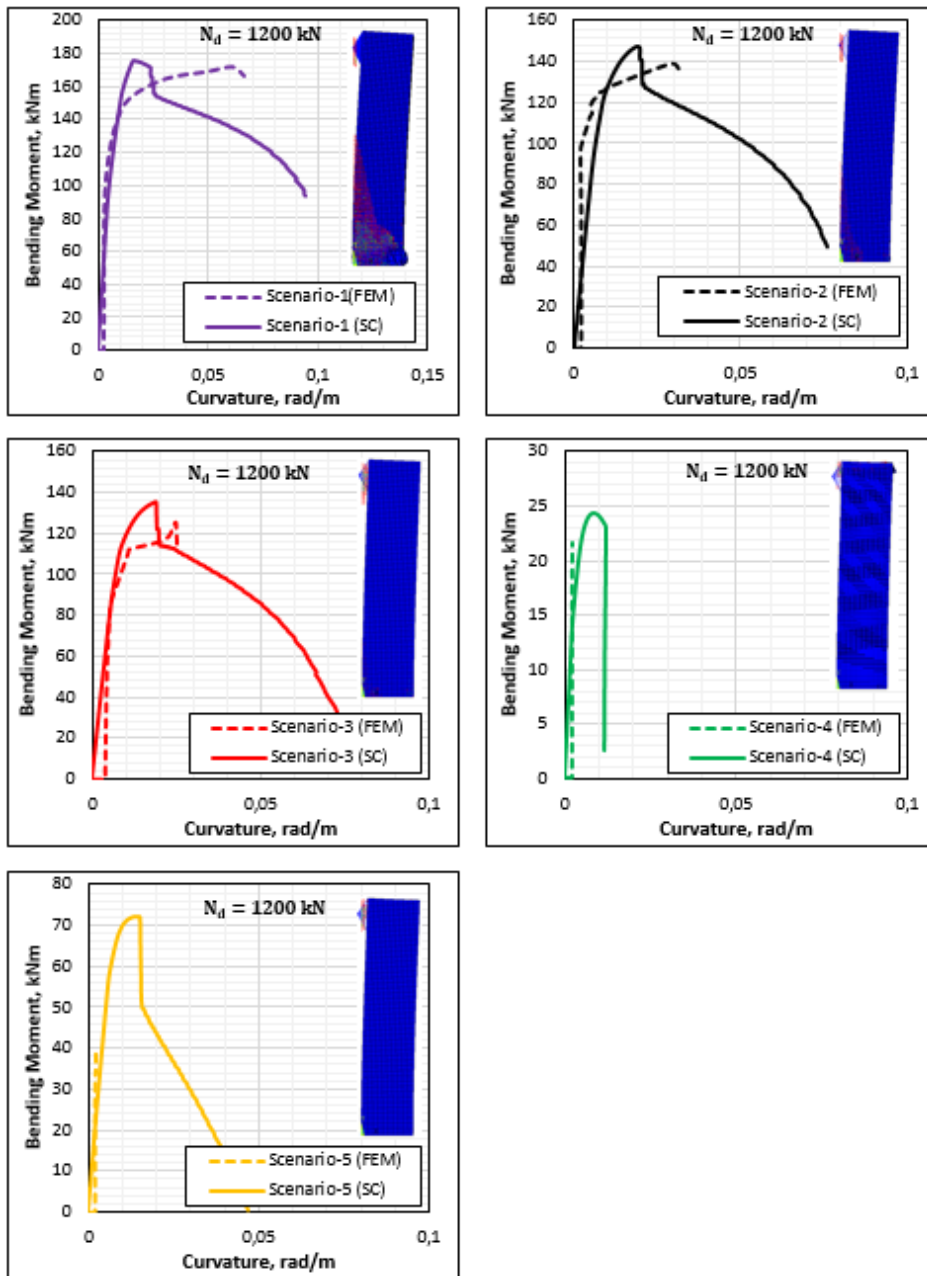


Figure 16. Bending moment – curvature relations for corrosion scenarios.

In Figure 16, the bending moment - curvature relationships of the reinforced concrete column subjected to corrosion effect in different corrosion scenarios compared in terms of nonlinear analysis and cross-sectional analysis, and in Table 4, the reduction in lateral load and bending moment carrying capacity for each corrosion level calculated according to Scenario-1 without corrosion effect.

3.2.1. Flexural ductility of reinforced concrete column

Flexural ductility defined as the ratio of the maximum curvature that can occur in a reinforced concrete element section in bending without a significant reduction in strength to the curvature now when yielding occurs in the tensile reinforcement, which is determined as the end of linear behavior. Flexural ductility calculated as shown in Equation 22 (Celep, 2008).

$$\mu = \frac{\phi_{u(max)}}{\phi_y} \tag{22}$$

The flexural ductility of the reinforced concrete column subjected to corrosion effect obtained because of nonlinear analysis and section analysis shown in Table 5.

3.2.2. Plastic joint yield rotation and plastic rotational capacity

As the reinforced concrete column element translated under the effect of the applied lateral load, the displacements increase at the sections where the moment is the largest at the base of the column. In particular, the displacements, which are zero at the place where the column supported on the foundation, increase smoothly until the plastic hinge occurs, while a sudden increase in curvature occurs in the plastic hinge region. Plastic joint yield rotation (θ_y) determined according to the stacked plastic behaviour model of the reinforced concrete column element is calculated as given in

Equation 23 and plastic rotation capacity (θ_p) is calculated as given in Equation 24, Equation 25 and Equation 26.

$$\theta_y = \frac{\phi_y L_s}{3} + 0.0015\eta \left(1 + 1.5 \frac{h}{L_s}\right) + \frac{\phi_y d_b f_{ye}}{8\sqrt{f_{ce}}} \tag{23}$$

$$\theta_p^{(G\ddot{o})} = \frac{2}{3} \left[(\phi_u - \phi_y) L_p \left(1 - 0.5 \frac{L_p}{L_s}\right) + 4.5\phi_u d_b \right] \tag{24}$$

$$\theta_p^{(KH)} = 0.75\theta_p^{(G\ddot{o})} \tag{25}$$

$$\theta_p^{(SH)} = 0 \tag{26}$$

Where ϕ_y the effective is yield curvature and ϕ_u is the total curvature before collapse. For beam and column elements, $\eta = 1$ taken and h is the height of the section. f_{ce} and f_{ye} are the average (expected) compressive strength of concrete and average yield strength of reinforcement, respectively. d_b is the average diameter of the reinforcing steel clamped to the support, while L_s is the shear span.

It assumed that the curvature in the plastic joint regions where linear inelastic deformations are concentrated in the reinforced concrete column subjected to corrosion effect increases abruptly. L_p , which expresses the length of the plastic joint region where the curvature increases rapidly, calculated as given in Equation 27.

$$L_p = 0.5h \tag{27}$$

Table 6 shows the plastic rotation capacities and plastic joint yield rotations of the reinforced concrete column for different corrosion scenarios in the nonlinear analysis and Table 7 shows the plastic rotation capacities and plastic joint yield rotations for Limited Damage (LD), Controlled Damage (CD) and Collapse Prevention (CP) performance levels in the section analysis.

Table 4. Lateral load and bending moment capacity losses

Scenario number	Lateral load (kN)		Bending moment (kNm)	
	FEM	SC	FEM	SC
Scenario -1	0.000		0.000	0.000
Scenario -2	20.99		18.95	15.79
Scenario -3	28.20		27.08	22.73
Scenario -4	87.96		87.37	86.05
Scenario -5	77.83		77.43	57.79

Table 5. Flexural ductility

Scenario number	Yield curvature (ϕ_y)		Maximum curvature ($\phi_{u(max)}$)		Flexural ductility (μ)	
	FEM	SC	FEM	SC	FEM	SC
Scenario -1	0.0078	0.011	0.060	0.094	7.69	8.55
Scenario -2	0.0061	0.0093	0.031	0.076	5.08	8.17
Scenario -3	0.0052	0.0085	0.024	0.073	4.62	8.58
Scenario -4	0.0021	0.0035	0.0022	0.012	1.05	3.43
Scenario -5	0.0022	0.0066	0.0023	0.047	1.05	7.12

Table 6. Plastic joint yield rotation and plastic rotational capacity (FEM)

Scenario number	Plastic rotation capacity			Plastic joint yield rotation
	$\theta_{P(SH)}$	$\theta_{P(KH)}$	$\theta_{P(GÖ)}$	(θ_y)
Scenario -1	0	0.01956	0.026079	0.008399
Scenario -2	0	0.009377	0.012503	0.007422
Scenario -3	0	0.007089	0.009453	0.006904
Scenario -4	0	0.000089	0.000119	0.005121
Scenario -5	0	0.000098	0.000131	0.005178

Table 7. Plastic joint yield rotation and plastic rotation capacity (SC)

Scenario no	Plastic rotation capacity			Plastic joint yield rotation
	$\theta_{P(SH)}$	$\theta_{P(KH)}$	$\theta_{P(GÖ)}$	(θ_y)
Scenario -1	0	0.031056	0.041408	0.010239
Scenario -2	0	0.024903	0.033204	0.009262
Scenario -3	0	0.024041	0.032054	0.008802
Scenario -4	0	0.00318	0.004239	0.005925
Scenario -5	0	0.015033	0.020044	0.007709

4. Discussion and Conclusion

In this study, the deformation of a rectangular reinforced concrete column subjected to corrosion effect under axial and lateral load effects investigated. In the study, the finite element model of the reinforced concrete column produced using ANSYS software and the nonlinear analysis performed. In addition, cross-sectional analysis of the reinforced concrete column under the effect of corrosion carried out and the deformation state compared with nonlinear analysis. The findings of the study draw attention to the losses caused by the corrosion effect on the lateral load carrying capacity and bending moment carrying capacity of the reinforced concrete column. In this context, it thought to be a good guide for the readers in determining the effect of corrosion on structures. The results obtained because of the research explained below.

- The lateral load and bending moment carrying capacities of reinforced concrete structural elements vary depending on the duration of the corrosion effect and the propagation speed parameters. Compared to Scenario-1, where there is no corrosion effect, in Scenario-4, where the corrosion effect is the most intense, the lateral load carrying capacity of the reinforced concrete column decreased by approximately 87.96% and the bending moment carrying capacity decreased by approximately 87.37% in the nonlinear analysis.
- When the Scenario-2 and Scenario-4 cases where the rate of corrosion spread is $i_{corr} = 4$ are examined, it is determined that the loss in the horizontal load and bending moment carrying capacity of the reinforced concrete column increases by an average of 4.4 times in the nonlinear analysis if the corrosion period increases from 20 years to 50 years.
- When Scenario-3 and Scenario-4 cases where the duration of corrosion is $t=50$ years, it is determined

that the loss in the horizontal load and bending moment carrying capacity of the reinforced concrete column increases by an average of 3.2 times in the nonlinear analysis if the corrosion propagation rate increases from 0.8 to 4.

- Ductility of reinforced concrete structural elements is of great importance in terms of earthquake performance. In this study, it was determined that corrosion effect not only reduces the lateral load and bending moment capacity of the reinforced concrete column but also negatively affects the flexural ductility. While the flexural ductility ratio was 7.69 according to the nonlinear analysis in Scenario-1 without corrosion effect, the flexural ductility ratio was determined as 1.05 in Scenario-4 with the highest corrosion effect. When the data obtained from the cross-sectional analysis of the reinforced concrete column are examined, it is determined that the flexural ductility ratio decreases significantly when the mass loss in the reinforcement increases to 35% and above due to the corrosion effect. It was determined that there was no significant change in the flexural ductility ratio as a result of the section analysis at mass losses below 35%. It is thought that this result is due to the fact that the section analysis does not consider the cracking behavior of concrete.
- In the nonlinear analysis of the reinforced concrete column, the plastic rotation capacity decreased by approximately 99.55 % for CD and CP damage limit levels in Scenario-4, where the corrosion effect is the highest, compared to Scenario-1, where there is no corrosion effect. In section analysis, this reduction was calculated as 89.76% for CD and CP damage limit levels in Scenario-4, where the mass loss in the reinforcement was more than 35%.
- In the beyond-linear analysis of the reinforced concrete column, it was determined that a loss of 12% for Scenario-2, 17% for Scenario-3, 17% for

Scenario-4 and 39% for Scenario-5 occurred in the plastic joint yield rotation value compared to Scenario-1 without corrosion effect. In the cross-sectional analysis, it was determined that a loss of 7% for Scenario-2, 11% for Scenario-3, 41% for Scenario-4 and 22% for Scenario-5 occurred in the plastic joint yield rotation value compared to Scenario-1. Accordingly, it can be said that similar losses occur in the plastic joint yield rotation value when the corrosion level is the highest in both nonlinear analysis and cross-sectional analysis.

- The bending moment capacity of the reinforced concrete column subjected to corrosion effect obtained from the nonlinear analysis was lower than the bending moment carrying capacity obtained from the cross-sectional analysis. The cracking property of the Solid65 element used in the finite element modelling under load effect and the cracking behavior of concrete are considered as the reason for this situation.

Author Contributions

The percentage of the author(s) contributions is presented below. All authors reviewed and approved the final version of the manuscript.

	H.E.Ç.	M.Ö.
C	50	50
D	60	40
S	40	60
DCP	50	50
DAI	40	60
L		100
W	100	
CR	40	60
SR	50	50
PM	50	50
FA	50	50

C=Concept, D= design, S= supervision, DCP= data collection and/or processing, DAI= data analysis and/or interpretation, L= literature search, W= writing, CR= critical review, SR= submission and revision, PM= project management, FA= funding acquisition.

Conflict of Interest

The authors declared that there is no conflict of interest.

Ethical Consideration

Ethics committee approval was not required for this study because of there was no study on animals or humans.

References

Berto L, Seatta A, Simioni P, Vitaliani R. 2008. Nonlinear static analyses of RC frame structures: influence of corrosion on seismic response. Proceedings of the 8th World Congress on Computational Mechanics (WCCM8), 23-25 June, Venice, Italy, pp: 25.

Berto L, Vitaliani R, Saetta A. 2009. Seismic assessment of

existing RC structures affected by degradation phenomena. *Struct Safety*, 31(4): 284-297.

Bhargava K, Ghosh AK, Yasuhiro M, Ramanujam S. 2008. Suggested empirical model for corrosion-induced bond degradation in reinforced concrete. *J Struct Eng*, 134(2): 221-230.

Bossio A, Imperatore S, Kioumars M. 2019. Ultimate flexural capacity of reinforced concrete elements damaged by corrosion. *Buildings*, 9(160): 1-13.

BRITE/EURAM. 1995. The residual service life of reinforced concrete structures, Final Technical Report, Report No. BRUE-CT92-0591.

Celep Z. 2008. Betonarme taşıyıcı sistemlerde doğrusal ötesi davranış ve çözümleme. İstanbul Teknik Üniversitesi, İstanbul, Türkiye, pp: 75.

Chung L, Kim JJ, Seong Y. 2008. Bond strength prediction for reinforced concrete members with highly corroded reinforcing bars. *Cement Concrete Compos*, 30 (7): 603-611.

Çolakoglu HE. 2020. Numerical investigation of the effect of transverse reinforcement spacing on earthquake performance of reinforced concrete columns. *Adiyaman Üniv Müh Bil Derg*, 12(7): 1-13.

Dhir RK, Jones MR, McCarthy MJ. 1994. PFA concrete: chloride-induced reinforcement corrosion. *Magazine Concrete Res*, 46(169): 269-277.

Dizaj EA, Kashani MM. 2021. Nonlinear structural performance and seismic fragility of corroded reinforced concrete structures: modelling guidelines, *European J Environ Civil Eng*, 2021: 5374-5403.

Elçi H, Göker KA. 2018. Comparison of earthquake codes (TEC 2007 and TBEC 2018) in terms of seismic performance of RC columns. *Int J Scient Technol Res*, 4(6): 9-21.

Ersoy U, Özcebe G. 2018. Betonarme. Orta Doğu Teknik Üniversitesi, Ankara, Türkiye, pp: 125.

Hsu TTC. 1993. Unified Theory of Reinforced Concrete. CRC-Press Inc., Boca Raton, US.

Imperatore S, Rinaldi Z, Drago C. 2017. Degradation relationships for the mechanical properties of corroded steel rebars. *Construct Build Mater*, 148: 219-230.

Lee HS, Cho YS. 2009. Evaluation of mechanical properties of steel reinforcement embedded in concrete specimen as a function of the degree of reinforced corrosion. *Int J Fracture*, 157(1): 81-88.

Mangat P, Elgarf M. 1999. Flexural strength of concrete beams with corroding reinforcement. *ACI Struct J*, 97(1): 149-59.

Middleton CR, Hogg V. 1998. Review of deterioration models used to predict corrosion in reinforced concrete structures. Cambridge University Engineering Department Technical Report No. CUED/D - STRUCT/TR.173, Cambridge, UK.

Mohammed TU, Hamada H, Yamaji T. 2004. Concrete after 30 years of exposure -Part II: Chloride ingress and corrosion of steel bars. *ACI Mater J*, 101(1): 13-18.

Molina FJ, Alonso C, Andrade C. 1993. Cover cracking as a function of rebar corrosion: part 2- numerical mode. *Mater Struct*, 26: 532-548.

Ou YC, Fan HD, Nguyen ND. 2013. Long-term seismic performance of reinforced concrete bridges under steel reinforcement corrosion due to chloride attack. *Earthquake Eng Struct Dynamics*, 42: 2113-2127.

Ou YC, Tsai MS, Chang KC, Lee G. 2010. Cyclic behavior of precast segmental concrete bridge column with high performance or conventional steel reinforcing bars as energy dissipation bars. *Earthquake Eng Struct Dynamics*, 39(11): 1181-1198.

Palsson R, Mirza MS. 2002. Mechanical response of corroded

- steel reinforcement of abandoned concrete bridge. *ACI Struct J*, 99(2): 157-162.
- Revathy J, Suguna K, Raghunath PN. 2009. Effect of corrosion damage on the ductility performance of concrete columns. *American J Eng Appl Sci*, 2(2): 324-327.
- Sezen H, Setzler EJ. 2008. Reinforcement slip in reinforced concrete columns. *ACI Struct J*, 105(3): 280-289.
- TBDY. 2018. Türkiye bina deprem yönetmeliği. Afet ve Acil Durum Başkanlığı, Ankara, Türkiye.
- Topçu A. 2022. Eskişehir Osmangazi Üniversitesi. URL: <http://mmf2.ogu.edu.tr/atopcu/> (accessed date: August 01, 2019).
- Vu NS, Li B. 2018. Seismic performance of flexural reinforced concrete columns with corroded reinforcement. *ACI Struct J*, 115(5): 1253-1266.
- Yavuz R, Günaydın O, Güçlüer K. 2019. Investigation of corrosion and adherence in reinforced concrete. *Kahramanmaraş Sütçü İmam Univ J Eng Sci*, 22: 12-18.
- Ying M, Yi C, Jinxin G. 2012. Behavior of corrosion damaged circular reinforced concrete columns under cyclic loading. *Construct Build Mater*, 29(1): 548-556.
- Yüksel İ, Sancaklı GB. 2018. Zemin katı korozyona maruz kalmış bir binanın performans değerlendirilmesi. *Eskişehir Teknik Üniv Bil Teknol Derg B- Teor Bil*, 6: 152-165.